Optimal fringe angle selection for digital fringe projection technique

Yajun Wang and Song Zhang*

Department of Mechanical Engineering, Iowa State University, Ames, Iowa 50011USA

*Corresponding author: song@iastate.edu

Received 10 June 2013; revised 5 September 2013; accepted 13 September 2013;
posted 13 September 2013 (Doc. ID 191969); published 3 October 2013

Existing digital fringe projection (DFP) systems mainly use either horizontal or vertical fringe patterns for three-dimensional shape measurement. This paper reveals that these two fringe directions are usually not optimal where the phase change is the largest to a given depth variation. We propose a novel and efficient method to determine the optimal fringe angle by projecting a set of horizontal and vertical fringe patterns onto a step-height object and by further analyzing two resultant phase maps. Experiments demonstrate the existence of the optimal angle and the success of the proposed optimal angle determination method. © 2013 Optical Society of America

OCIS codes: (120.0120) Instrumentation, measurement, and metrology; (120.2650) Fringe analysis; (100.5070) Phase retrieval.

http://dx.doi.org/10.1364/AO.52.007094

1. Introduction

Three-dimensional (3D) shape measurement is of great importance to fields ranging from manufacturing to medicine [1,2]. Numerous techniques have been developed, including Moiré, holography, and digital fringe projection (DFP) [3]. Among these 3D shape measurement methods, the DFP techniques have become mainstream and more widely adopted due to their simple setup, high speed, and high-resolution measurement capabilities [4,5].

Conventionally, a DFP system uses a projector to project horizontal and/or vertical fringe patterns onto the surface of the object to be measured [6–8]. By analyzing the captured distorted fringe images using a camera, the phase map can be obtained, from which the 3D depth information can be further retrieved, if the system is calibrated. It is well known that the design of such a system is usually not easy and often involves complicated trial-and-error procedures. The optimal design will essentially provide the best sensitivity to depth variation; in other words, the phase changes are largest for a given depth variation (i.e., maximize $\partial\Phi/\partial z$). To our knowledge, no attention has been paid toward orienting the projected fringe patterns such that the system can achieve optimal performance.

This paper will reveal that the fringe angle plays a vital role in determining the optimal performance of the 3D shape measurement system with a DFP technique, and simply projecting horizontal or vertical fringe patterns may not be the best option. It becomes crucial to determine the optimal fringe angle for a given system setup without changing its mechanical design; here, a novel and efficient method to determine the optimal fringe angle is proposed. Specifically, by projecting a set of horizontal and vertical fringe patterns onto a step-height object, we obtain two phase maps, from which the phase differences between the top and the bottom surfaces of the step height objects can be calculated. Finally, the mathematical vector operation on these phase differences can be used to determine the optimal projection angle. Our further studies indicate that if the projected fringe stripes have the optimal angle, the phase is the most sensitive to depth variations. Conversely, if the fringe stripes are perpendicular

1559-128X/13/297094-05$15.00/0

to the optimal fringe direction, the system is the least sensitive to depth variations.

2. Phase-Shifting Algorithm

Phase-shifting methods are widely used in optical metrology because of their speed and accuracy [9]. A three-step phase-shifting algorithm with equal phase shifts can be described as

$$I_1(x,y) = I'(x,y) + I''(x,y)\cos(\phi - 2\pi/3), \quad (1)$$

$$I_2(x,y) = I'(x,y) + I''(x,y)\cos(\phi), \quad (2)$$

$$I_3(x,y) = I'(x,y) + I''(x,y)\cos(\phi + 2\pi/3), \quad (3)$$

where $I'(x,y)$ is the average intensity, $I''(x,y)$ the intensity modulation, and $\phi(x,y)$ the phase to be solved for. Simultaneously solving Eqs. (1)–(3) leads to

$$\phi(x,y) = \tan^{-1}\left[\sqrt{3}(I_1 - I_3)/(2I_2 - I_1 - I_3)\right]. \quad (4)$$

The arctangent function generates the phase value, ranging $[-\pi, +\pi)$ with 2π discontinuities. A spatial phase unwrapping algorithm [10] can be used to remove the 2π discontinuities, but has problems when the object surface has abrupt changes, or contains multiple isolated patches. This research adopted the multi-frequency algorithm, using a temporal phase unwrapping algorithm to obtain the absolute phase map, $\Phi(x,y)$ [11].

3. Optimal Fringe Angle Selection

A DFP system usually contains a digital video projection unit, a digital camera imaging unit, and a fringe processing or analysis unit. In a conventional DFP system, the computer generated fringe patterns are usually either horizontal or vertical, which are then projected by the video projector onto the object's surface. The fringe patterns captured by he camera are then analyzed by the computer to obtain the phase map, which can be further converted to 3D shape information once the system is calibrated. However, our research found that simply projecting horizontal or vertical fringe patterns might not be *optimal* if the camera and the projector are not positioned perfectly. Here, optimal performance means that the system is the most sensitive to the depth changes on the object's surface, i.e., $\partial\Phi/\partial z$ is the largest for a given setup.

It should be noted that the projected patterns generated by a computer can be perfectly horizontal or vertical, but the captured fringe patterns by the camera may have small angle error (i.e., the fringe patterns may not be perfectly horizontal or vertical). The proposed optimal fringe angle determination method was based on the computer generated fringe patterns before sending to the projector, and thus the angle error can be considered negligible. Practically, if the projected fringe patterns are close to the optimal angle, the phase change is nearly the largest with a given depth variation. In contrast, if the fringe angle is close to being perpendicular to the optimal angle, the phase change is close to being zero with the same depth change, meaning that the measurement sensitivity is very low and the measurement accuracy is drastically jeopardized due to factors such as system noise and/or phase error.

To achieve high sensitivity, one can adjust the relative position and orientation between the projector and the camera, which is usually not easy. Instead of mechanically redesigning the system, we propose to change the projected fringe stripe orientation such that the system can achieve the best sensitivity. Specifically, we propose the following procedures to determine the optimal fringe angle:

(1) Project horizontal and vertical fringe patterns onto a step-height object and a uniform flat reference plane; then, obtain these four absolute phase maps by employing a multi-frequency phase-shifting algorithm: (a) horizontal absolute phase map of the object Φ_{Ho}, (b) vertical absolute phase map of the object Φ_{Vo}, (c) horizontal absolute phase map of the reference plane Φ_{Hr}, and (d) vertical absolute phase map of the reference plane Φ_{Vr}.

(2) Calculate the difference phase maps by subtracting the object phase maps with the corresponding reference phase maps

$$\Delta\Phi_{\mathrm{Hd}} = \Phi_{\mathrm{Ho}} - \Phi_{\mathrm{Hr}}, \quad (5)$$

$$\Delta\Phi_{\mathrm{Vd}} = \Phi_{\mathrm{Vo}} - \Phi_{\mathrm{Vr}}. \quad (6)$$

(3) Compute the phase difference between top and bottom surfaces of the step-object using the following equations

$$\Delta\Phi_H = \Delta\Phi^t_{\mathrm{Hd}} - \Delta\Phi^b_{\mathrm{Hd}}, \quad (7)$$

$$\Delta\Phi_V = \Delta\Phi^t_{\mathrm{Vd}} - \Delta\Phi^b_{\mathrm{Vd}}. \quad (8)$$

(4) Determine the optimal fringe angle using the following equation, which is illustrated in Fig. 1

$$\theta_o = \tan^{-1}[\Delta\Phi_V/\Delta\Phi_H]. \quad (9)$$

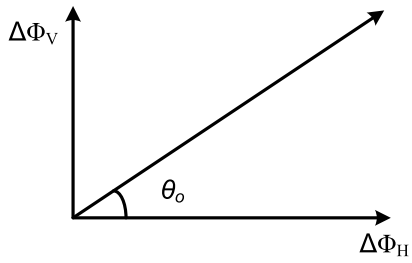

Fig. 1. Calculation of the optimal fringe angle.

This is essentially the angle of the vector $\vec{v} = \Delta\Phi_H\vec{i} + \Delta\Phi_V\vec{j}$. Here, $\vec{i}$ and $\vec{j}$ are the unit vectors along the x and y axes, respectively.

As explained previously, if the projected fringe patterns use the optimal angle θ_o, the phase change is greatest with the same amount of depth variation. Therefore, such a system can be used to measure the smallest features on an object surface for a given hardware system configuration. This finding is especially valuable for a DFP system where the orienting of the projected fringe patterns can be easily realized.

4. Experimental Results

We implemented such an optimal angle determination method to a DFP system. The system includes a digital-light-processing (DLP) projector (Samsung SP-P310MEMX) and a digital CCD camera (Jai Pulnix TM-6740CL). The camera uses a 16 mm focal length Mega-pixel lens (Computar M1614-MP). The camera resolution is 640×480, with a maximum frame rate of 200 frames/sec. The projector has a resolution of 800×600 with a projection distance of 0.49–2.80 m.

We use a standard step-height block to determine the optimal angle of our DFP system. The block size is approximately 40 mm(H) × 40 mm(W) × 40 mm(D). Figure 2 shows the measurement results using horizontal and vertical fringe patterns. Figures 2(a) and 2(d), respectively, show one of the horizontal and vertical fringe images captured by the camera. Figures 2(b) and 2(e) show the corresponding phase difference maps (Φ_{Hd} and Φ_{Vd}), which were obtained using Eqs. (5) and (6). To better illustrate the phase difference maps, Figs. 2(c) and 2(f), respectively, show the same cross section of the phase map as those shown in Figs. 2(b) and 2(e).

Taking the difference between the top surface of the block and the bottom surface of the block, we obtain $\Delta\Phi_H$ and $\Delta\Phi_V$, from which we can determine the optimal angle (θ_o) using Eq. (9). It should be noted that we used the averaged phase values for the phase difference determination on the step-height object to alleviate the noise effect. Namely, we averaged the phase maps of a small area on the top surface and that on the bottom surface to calculate the phase difference for each fringe angle. In this case, the optimal fringe angle is approximately ($\theta_o = -0.73$ rad). In contrast, if the fringe stripe is perpendicular to the optimal fringe stripe direction, the system is the least sensitive to depth changes. In other words, if the fringe angle $\theta = 0.84$ rad, the phase difference map of the step-height block should be close to zero.

We then experimentally verified the optimal angle we had determined; Fig. 3 shows the results. Figures 3(a) and 3(d), respectively, show one of the captured fringe images under the worst and optimal fringe angles. Figures 3(b) and 3(e) show the corresponding phase difference maps. The cross sections are shown in Figs. 3(c) and 3(f). These experiments show that the phase difference is indeed close to zero if the fringe direction is perpendicular to the optimal fringe direction; and when the projected patterns use the optimal fringe angle, the phase difference

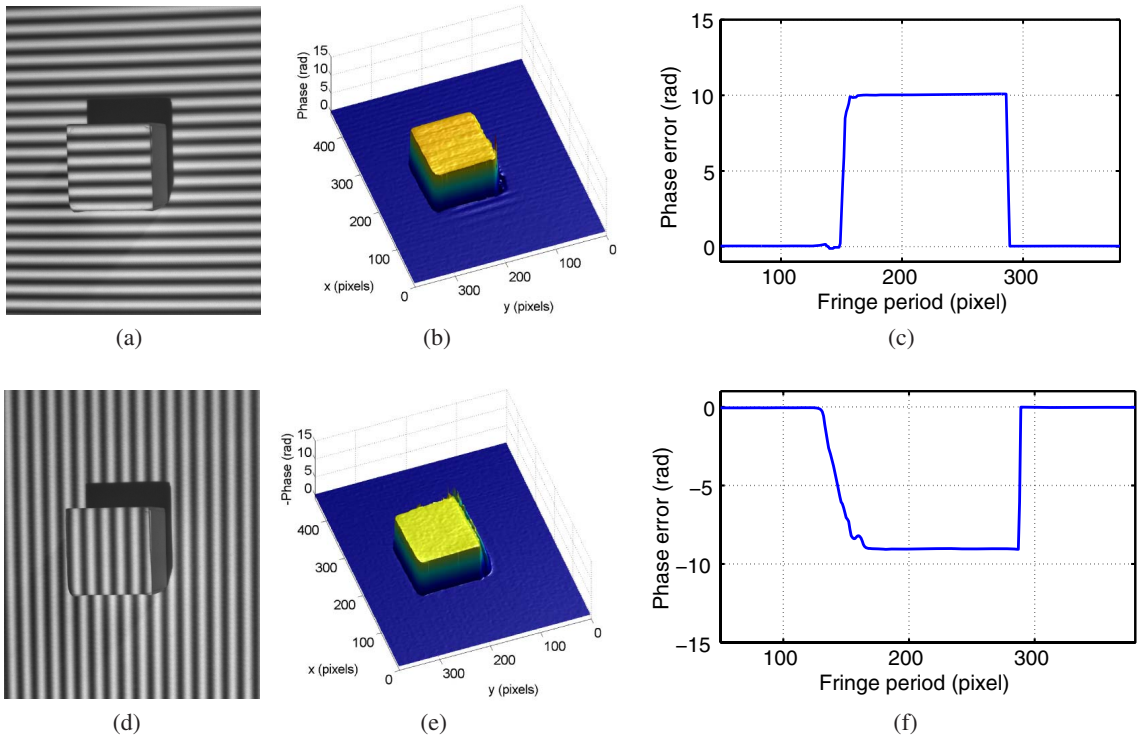

Fig. 2. Phase measurements using horizontal and vertical fringe patterns. (a) One of the captured horizontal fringe patterns. (b) Phase difference map Φ_{Hd} and (c) 250th row cross section of (b). (d) One of the captured horizontal fringe patterns. (e) Phase difference map Φ_{Vd} and (f) 250th row cross section of (e).

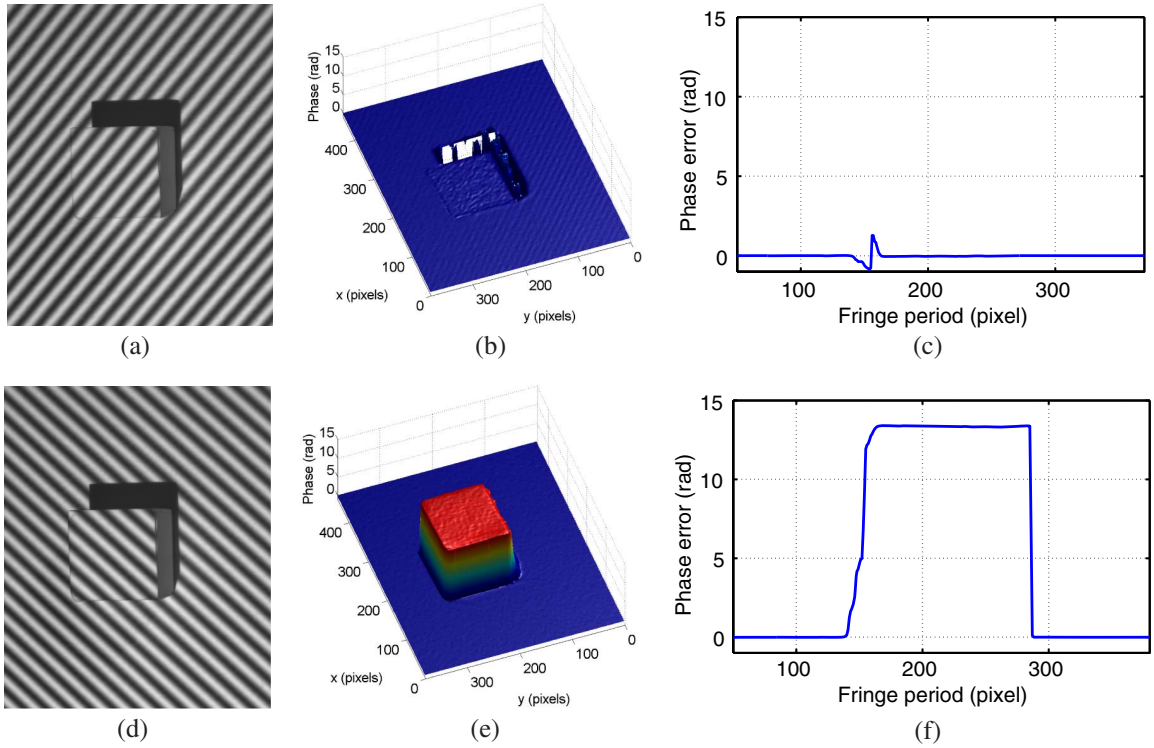

Fig. 3. Results for the fringe patterns with the worst and the optimal fringe angles. (a) One of the captured fringe images with $\theta = 0.84$ rad, the worst fringe angle. (b) Phase difference map of (a) and (c) 250th row cross section of (b). (d) One of the captured fringe images with $\theta_o = -0.73$ rad, the optimal fringe angle. (e) Phase difference map of (d) and (f) 250th row cross section of (e).

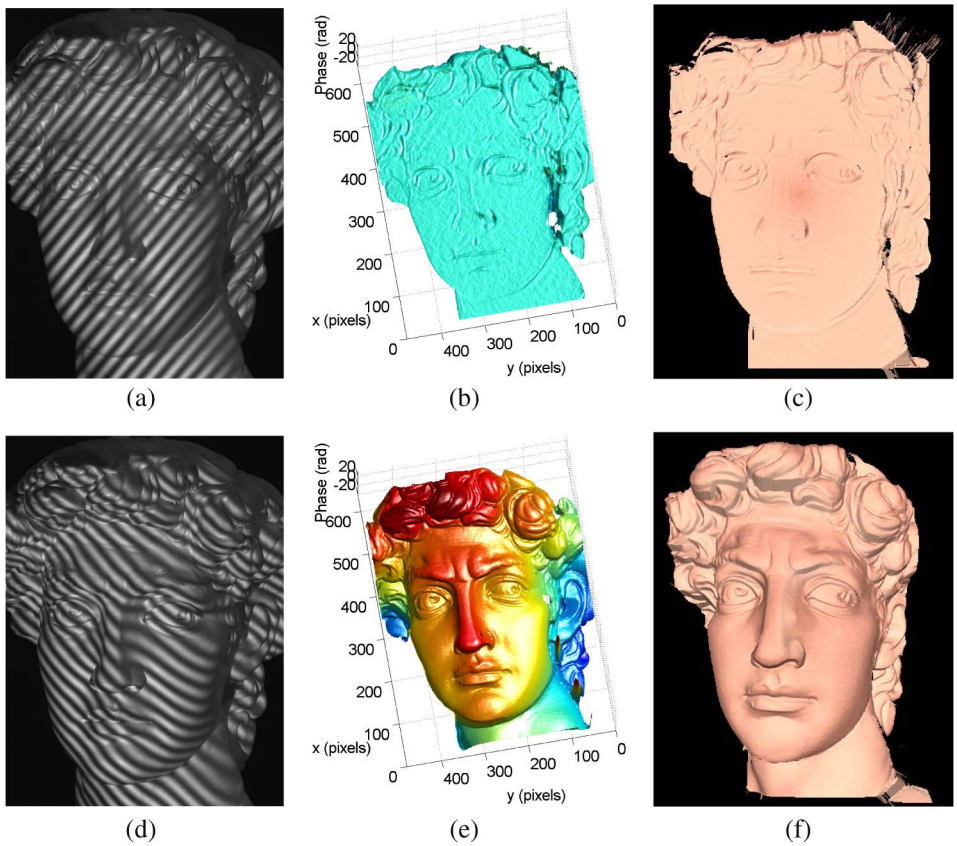

Fig. 4. Sculpture results under different fringe angles. (a) One of the captured fringe patterns with the worst fringe angle $\theta = 0.84$ rad. (b) Phase difference map ($\theta = 0.84$ rad). (c) Recovered 3D shape ($\theta = 0.84$ rad). (d) One of the captured fringe patterns with the optimal fringe angle $\theta_o = -0.73$ rad. (e) Phase difference map ($\theta_o = -0.73$ rad). (f) Recovered 3D shape ($\theta_o = -0.73$ rad).

is drastically larger than either the horizontal or the vertical fringe patterns we normally use, as illustrated in Fig. 2. It should be noted that, during all experiments, the whole hardware system remained untouched; the object was positioned in the same location, and the fringe period was the same. These data demonstrate that we can determine the optimal fringe angle, and that, under optimal conditions, the system is the most sensitive to depth variation.

A more complex sculpture was also measured using the optimal fringe angle and the worst fringe angle, as shown in Fig. 4. Figures 4(a) and 4(d) show one of the captured fringe patterns and Figs. 4(b) and 4(e) show the corresponding phase difference maps. It can be seen that the phase difference map is nearly flat, and no details are obvious on Fig. 4(b), when the worst fringe angle is used. In contrast, Fig. 4(e) clearly shows the highly detailed features on the difference map when the fringe patterns use the optimal fringe angle. We further convert phase difference maps to depth maps using the simple phase-to-height conversion algorithm discussed in [12]. The depth scaling coefficient was obtained using the optimal fringe angle, and applied to both phase difference maps. Figures 4(c) and 4(f), respectively, show the worst and the best results; clearly, when using the optimal fringe angle, the 3D object can be properly measured in detail. Yet, if the fringe orientation rotates 90 degrees, the 3D shape cannot be properly recovered at all, since the phase difference map is close to zero across the whole range.

5. Discussion

As demonstrated in Section 4, phase sensitivity is significantly improved when the optimal angle is used. Theoretically, if the system is perfectly linear and the fringe angle is perpendicular to the optimal fringe angle, no 3D shape measurement can be performed, since the fringe patterns will not be distorted by object surface geometry; and, if no noise is present in the measurement system, even if the fringe angle is not optimal, the measurement accuracy will probably not be changed. However, practically, noise is always presents, and the measurement accuracy could be affected by the fringe angle.

Assume the phase error caused by the system noise is $\delta\Phi_e$, which is the same once the system is set up for a given phase-shifted fringe pattern. For a simple reference-plane-based calibration method, the relationship between the depth z and the phase difference is $z = z_0 + c \times \Delta\Phi$ [12]; here, z_0 is the constant shift and c is the calibration constant. Therefore, the depth error caused by system noise is approximately $\Delta z_e = c \times \delta\Phi_e$. This indicates that the larger the calibration constant, the larger the measurement error that will be induced by noise (i.e., a lower measurement accuracy will be achieved). When the phase sensitivity ($\partial\Phi/\partial z$) is higher, the calibration constant c is smaller, and thus depth measurement accuracy is higher.

One may notice that Chen *et al.* [13] proposed a method to enhance measurement quality by avoiding the frequency aliasing of Fourier transform profilometry (FTP) by changing fringe orientations. The objective of that paper was to avoid frequency aliasing. Since the frequency spectrum is also affected by the object surface geometry, the fringe angle determined by such an approach depends on not only the system setup, but also the object surface geometry. Therefore, the optimal fringe orientation should be determined for each individual measurement object. In contrast, our paper is a systematic approach that is completely independent of the measured object surface geometry. Once the system is set up, the optimal angle can be determined using the proposed approach.

6. Conclusion

We have presented a novel and effective method to determine the optimal fringe angle for a DFP technique. Experimental results have demonstrated the feasibility of the proposed method, and the capability of the proposed method to enhance phase sensitivity to depth variations.

This study was partially funded by the National Science Foundation under the project numbers CMMI-1150711 and CMMI-1300376.

References

1. C. Quan, C. J. Tay, X. Y. He, X. Kang, and H. M. Shang, "Microscopic surface contouring by fringe projection method," Opt. Laser Technol. **34**, 547–552 (2002).
2. A. Hanafi, T. Gharbi, and J. Cornu, "In vivo measurement of lower back deformations with Fourier-transform profilometry," Appl. Opt. **44**, 2266–2273 (2005).
3. S. Zhang, ed., *Handbook of 3D Machine Vision: Optical Metrology and Imaging*, 1st ed. (CRC Press, 2013).
4. S. Gorthi and P. Rastogi, "Fringe projection techniques: whither we are?" Opt. Laser Eng. **48**, 133–140 (2010).
5. G. Geng, "Structured-light 3D surface imaging: a tutorial," Adv. Opt. Photon. **3**, 128–160 (2011).
6. X. Su and W. Chen, "Fourier transform profilometry: a review," Opt. Laser Eng. **35**, 263–284 (2001).
7. P. Huang and S. Zhang, "Fast three-step phase-shifting algorithm," Appl. Opt. **45**, 5086–5091 (2006).
8. Q. Zhang and X. Su, "High-speed optical measurement for the drumhead vibration," Opt. Express **13**, 3110–3116 (2005).
9. D. Malacara, *Optical Shop Testing*, 3rd ed. (Wiley, 2007).
10. D. C. Ghiglia and M. D. Pritt, *Two-Dimensional Phase Unwrapping: Theory, Algorithms, and Software* (Wiley, 1998).
11. Y. Wang and S. Zhang, "Superfast multifrequency phase-shifting technique with optimal pulse width modulation," Opt. Express **19**, 5143–5148 (2011).
12. Y. Xu, L. Ekstrand, J. Dai, and S. Zhang, "Phase error compensation for three-dimensional shape measurement with projector defocusing," Appl. Opt. **50**, 2572–2581 (2011).
13. W. Chen, X. Su, Y. Cao, L. Xiang, and Q. Zhang, "Fourier transform profilometry based on a fringe pattern with two frequency components," Optik **119**, 57–62 (2008).